Int. J. Mach. Tools Manufact. Vol. 32, No. 4, pp.495–508, 1992.
Printed in Great Britain

0890-6955/92$5.00 + .00

MODELLING OF MULTIVARIATE TIME SERIES FOR TOOL WEAR ESTIMATION IN FINISH-TURNING

Y. YAO† and X. D. FANG‡

(*Received* 7 *March* 1991; *in final form* 11 *July* 1991)

Abstract—In finish-turning, the traditional flank or crater wear estimation alone is no longer adequate, whilst the wear at the minor cutting edge is of primary concern since it directly affects the surface quality and dimensional accuracy of a finished product. This paper describes the development of an overall tool wear monitoring strategy in finish-turning. To estimate various types of wear developing at the different faces of a tool insert, multidimensional force and vibration signals are used, and a stochastic technique, based on multivariate autoregressive moving average vector models (ARMAV), is used to quantify the process dynamics embedded in the signals. Based on that, a dispersion analysis is carried out to discriminate among signal ingredients each of which is sensitive to a particular type of wear. Experimental results show that the groove wear at the minor cutting edge, once formed, dominates the finishing-tool life, while in the case of no groove formation at the minor cutting edge, the minor flank wear reaches its critical point earlier than the major flank or crater wear does. The results also show that the method derived from the dispersion analysis is a feasible approach to on-line tool wear estimation in finish-turning.

1. INTRODUCTION

IN AUTOMATED machining, on-line tool wear estimation plays an important role in establishing an efficient tool change policy and effective quality control strategy. Numerous methods have been developed, as reviewed in several survey papers [1–4]. Most of them, however, are concerned with the estimation of the major flank wear alone [5–14] or with the major flank and crater wear combined [15–18]. In actual machining operations, especially in a finish-turning process, the minor flank wear, groove wear at the minor cutting edge and nose wear are crucial to dimensional accuracy and surface finish. It is likely that in finish-turning, the wear state at the minor cutting edge reaches its critical point earlier than those in the major flank and crater, such that the tool monitoring policy should be set based on the wear state at the minor cutting edge. Therefore, a more effective monitoring strategy involving multi-sensor and/or multi-modelling is called for in order to estimate more than one type of tool wear simultaneously.

The mechanism of minor flank wear and groove wear at the minor cutting edge is complex. The minor flank wear will always form in the machining process, while under certain cutting conditions, the grooves, spaced at a distance equal to feed, may appear and become the dominant wear at the minor cutting edge. When no grooves form at the minor cutting edge, the machined workpiece surface is further shaped by the minor cutting edge, thus causing minor flank wear mainly due to high-speed friction. The surface finish and dimensional accuracy are affected by the severity of minor flank wear. When the grooves are formed at the minor cutting edge under certain cutting conditions, the surface roughness is primarily determined by the depth of these grooves [19].

Although the minor flank wear and groove wear at the minor cutting edge have been recognized long ago to be crucial to the surface quality in finish-machining and much work has been done on their mechanism [20–24], almost no work has been reported on the detection and estimation methods for these types of tool wear, presumably due to the complexity involved in interpreting multivariate signals and resolving them for estimation of more than one type of wear.

†School of Mechanical and Manufacturing Engineering, University of New South Wales, NSW 2033, Australia.
‡Department of Mechanical Engineering, University of Wollongong, NSW 2500, Australia.

Autoregressive moving average (ARMA) time series analysis techniques have been used in modelling machining processes during the past decade. As it does not require much prior knowledge about the underlying system physics, ARMA modelling is most suitable for cutting processes which are stochastic in nature. By using the ARMA modelling techniques, a mathematical model which describes the internal system dynamics can be established based solely on experimentally measured data. Once the ARMA models are established, the feature extraction can be developed in different ways, such as residual analysis [25], parametric spectral analysis [26, 27], dispersion analysis [26, 28–30], damping ratio calculation [7, 31], model parameters [5, 6, 32], etc. When more than one series of data are involved, multivariate ARMA vector models [28, 30, 33] may be developed to reveal the interactive characteristics between different series. Table 1 summarizes applications of ARMA modelling in on-line monitoring concerning machining processes.

As seen from Table 1, most methods use only the univariate time series model to estimate tool wear. If more than one quantity is to be estimated, more complexity will be encountered. Thus, a higher demand is placed on effective signal processing and analysis techniques which shall be able to single out particular signal ingredients sensitive to particular quantities to be estimated. This paper describes an investigation into comprehensive tool wear estimation in finish-machining of a bar. The dispersion analysis algorithm based on multivariate ARMA vector models was developed, leading to the effective discrimination between various modes of variables in a quantitative way.

2. DISPERSION ANALYSIS BASED ON MULTIVARIATE ARMA VECTOR MODEL

2.1. *Modelling of multivariate time series*

Multivariate time series ARMA vector models were developed to analyse the dynamic relationship among the data collected from the machining process, such as 3-D dynamic cutting forces or 3-D tool vibrations. When a dynamic process, represented by its p-dimensional components is sampled at a uniform interval, Δ, the resulting discrete

TABLE 1. ARMA MODELLING OF MACHINING PROCESSES FOR CONDITION MONITORING

References	Year	Specifications of application	Signals used	Model dimensions	Diagnostic methods and feature extraction
[5]	1987	major flank wear estimation	AE	1-D	model parameters
[6]	1989	major flank wear estimation	AE	1-D	model parameters
[7]	1980	major flank wear estimation	vibration	1-D	damping ratio
[8]	1982	major flank wear estimation	2-D forces and 1-D vibration	1-D	actual power contribution of ARMA spectral analysis
[25]	1986	tool breakage detection	cutting torque	1-D	residual analysis
[26]	1980	on-line identification of chatter in turning process	2-D vibration and cutting forces	1-D	autoregressive spectral density and dispersion analysis
[27]	1990	estimations of crater wear and minor flank wear	3-D dynamic cutting forces	3-D	autoregressive spectral analysis
[28]	1990	comprehensive tool wear estimation in finish-turning	3-D dynamic cutting forces	3-D	dispersion analysis
[29]	1977	chatter identification	vibration	1-D	dispersion analysis
[30]	1991	estimation of groove wear at the minor cutting edge	3-D vibration	3-D	multiple dispersion analysis
[31]	1985	estimation of average flank wear in drilling process	thrust torque	1-D	normalized damping ratio
[32]	1986	tool breakage detection in milling process	cutting force	1-D	prediction errors based on model parameters

series of observation vectors $\mathbf{X}_t$, $t=1,2,\ldots,N$, can be represented by a p-variate ARMA vector model of autoregressive order n and moving average order m, denoted by ARMAV(n,m):

$$\mathbf{X}_t = \sum_{i=1}^{n} \Phi_i \mathbf{X}_{t-i} + \mathbf{a}_t - \sum_{i=1}^{m} \theta_i \mathbf{a}_{t-i} \tag{1}$$

where the p-dimensional vector $\mathbf{X}_t = [X_{1t}, X_{2t}, \ldots, X_{pt}]^T$, is expressed as a linear combination of past observation vectors $\mathbf{X}_{t-i}$, $i=1,2,\ldots,n$, and independent random vector $\mathbf{a}_t = [a_{1t}, a_{2t}, \ldots, a_{pt}]^T$, and a_{t-i}, $i=1,2,\ldots,m$.

The parameter matrices Φ_i and θ_i, estimated based on the observation vectors, describe the instantaneous dynamics of the machining process. The orders of an adequate model can be determined by the F-test and an ARMAV(n,m) model can be approximated by an autoregressive model, i.e. ARV(n) with a sufficiently high order [33]. An ARV(n) model requires much less computation than the ARMAV model, such that it is more attractive to on-line implementations. When applied to the oblique machining process, an ARV(n) model has a much simpler form:

$$\mathbf{X}_t = \sum_{i=1}^{n} \Phi_i \mathbf{X}_{t-i} + \mathbf{a}_t \tag{2}$$

where $\mathbf{X}_t = (X_{1t}, X_{2t}, X_{3t})^T$

$$\Phi_i = \begin{pmatrix} \Phi_{11i} & \phi_{12i} & \Phi_{13i} \\ \Phi_{13i} & \Phi_{22i} & \phi_{23i} \\ \Phi_{31i} & \Phi_{32i} & \Phi_{33i} \end{pmatrix} \text{ and } \mathbf{a}_t = (a_{1t}, a_{2t}, a_{3t})^T .$$

2.2. *Dispersion analysis*

After an adequate ARMAV model is determined, the dispersion analysis can be introduced to discriminate among various modes of process variations in a quantitative way. It has been shown [33] that the total process variance can be represented by the contributions (d_i) due to each variation mode of the process eigenvalues, λ_i, ($i=1,2,\ldots,n$, for each series) as follows:

$$\gamma_0 = E[\mathbf{X}_t \mathbf{X}_t^T] = \sum_{i=1}^{n} d_i = \sum_{i=1}^{n} g_i \sum_{k=1}^{n} \frac{\sigma_a g_k}{1 - \lambda_i \lambda_k} \tag{3}$$

where d_i is the dispersion associated with eigenvalue λ_i and g_i is calculated by the following equation:

$$g_i = \frac{\lambda_i^{n-1}}{\prod_{k=1, k\neq i}^{n} (\lambda_i - \lambda_k)} . \tag{4}$$

The dispersion percentage, D_i, describes the contribution of the roots or ultimately the frequencies in the series to the series variation γ_0, and is given as:

$$D_i = \frac{d_i}{\gamma_0} . \tag{5}$$

In this way, the process variation γ_0 is decomposed into contributions of process eigenvalues in terms of dispersion (D_i) quantitatively. Of particular interest are the dispersion percentages (D_i) associated with eigenvalues (λ_i) occurring in complex conju-

gate pairs (λ_1 and λ_2) which describe the oscillating variation of the machining process. The frequency corresponding to a pair of complex conjugate eigenvalues is given in Ref. [33]:

$$f_n\,(\mathrm{Hz}) = \frac{1}{2\pi\Delta}\sqrt{\frac{[\ln(\lambda_1\lambda_2)]^2}{4} + \left[\cos^{-1}\left(\frac{\lambda_1+\lambda_2}{2\sqrt{\lambda_1\lambda_2}}\right)\right]^2} \tag{6}$$

where Δ is the sample interval in seconds. The significance of dispersion analysis lies in that the relative importance of the oscillating mode of each existing frequency can be established such that analysis and interpretation in terms of physical phenomena, such as natural frequencies of the tool/tool holder system and machine tool structural frequencies, can be carried out in a quantitative manner.

3. MAJOR FLANK, CRATER AND MINOR FLANK WEAR ESTIMATION

Since groove formation at the minor cutting edge occurs only under certain cutting conditions, minor flank wear is first estimated along with major flank and crater wear. It has been shown that using a 3-D dynamic cutting force is an effective means for providing necessary information about wear states at different tool faces.

3.1. *Description of experiments*

Since in finish-turning, tool wear to be estimated is on different faces of a tool, the 3-D dynamic cutting forces were used. This is also because the dynamic component contains richer information about tool/workpiece interactions than the cutting force itself. The three orthogonal dynamic components of the cutting forces were measured by using a tool dynamometer (KISTLER 9257A). Four typical cutting conditions were selected for tool wear experiments, as shown in Table 2. As we are only interested in the development patterns of particular types of tool wear, the degraded tool tests, i.e. using relatively softer tools as recommended in Ref. [34], are adopted to shorten the time-consuming and costly tool wear experiments.

In order to simulate the experimental conditions as close as possible to practical machining operations, the machining process was interrupted periodically with an increment of about 5 min under cutting condition group 1 and about 2.5 min under groups 2–4. The tool was replaced by a fresh one at each interruption such that every tool remained in thermal continuity until it was replaced. Just before each tool replacement, a set of 524 data points was sampled for each channel. Therefore, the experimental results consist of 7 tools and 7 sets of data from each channel under all four groups of cutting conditions. Before the dynamic cutting force, in terms of its three orthogonal components, were sampled into a multi-channel data acquisition system with a sample interval equal to 60 μs (about 16.7 kHz), low-pass filters with a cut-off frequency of 4 kHz were applied, considering the 4 kHz natural frequency of the dynamometer.

TABLE 2. MACHINING CONDITIONS USED IN TOOL WEAR EXPERIMENTS

Machine tool	Colchester Mascot 1600 (9.3 kW)
Tool insert type	TNMA 160408F (Carbide: Grade 883, SECO)
Tool geometry	0°, 5°, −6°, 90°, 60°, 0.8
Work material	AISI4140 (HNB=320)
Workpiece size	Length = 1m and Diameter = 100mm
Cutting conditions	1. V=115 m/min f=0.1 mm/rev d=0.5 mm
	2. V=145 m/min f=0.1 mm/rev d=0.5 mm
	3. V=145 m/min f=0.06 mm/rev d=0.5 mm
	4. V=145 m/min f=0.06 mm/rev d=0.25 mm
Cutting fluid	No

3.2. *Tool wear measurement and wear development patterns*

The scanning electron microscope (SEM), stereo microscope with camera attachment, surfcom (a surface roughness instrument) and coordinate measuring machine (CMM) were used jointly to measure wear parameters. Figure 1 shows a typical group of tool wear photographs taken by SEM, indicating the wear situations on different tool faces. Four major wear parameters, including major flank wear VB, crater depth KT, minor flank wear VB' and nose wear N, are selected in accordance with CIRP tool wear terminology [19] to describe tool wear states. The groove wear (see Fig. 1(d)) at the minor cutting edge was not selected because of its inconsistent appearance under the machining conditions used in the experiment and it will be addressed separately in a later section. All the measurement results of the four types of tool wear were plotted in Figs 2–5, respectively, for all four groups of cutting conditions. It is interesting to observe that except nose wear, N, all types of tool wear have an accelerating stage, as indicated in the figures.

3.3 *Analysis based on the dispersion patterns*

In parallel to the measurement of various types of wear, the 3-D dynamic cutting force was modelled using the ARMAV technique described before. As a result of the analysis of the dispersion patterns for all corresponding frequencies, it was found that there exist two dominant dispersions, d_i, i.e. the two largest percentage D_i values, with the most significant one associated with a lower frequency (LF) range and the second most significant one with a higher frequency (HF) range. The dominant dispersions for all the first three cutting conditions are plotted in Figs 6–8.

The dispersion trends shown in Figs 6–8 were then correlated to the rate of the various types of wear presented in Figs 2–5, followed by physical interpretation. Since the forces acting on different tool faces are projected to the 3-D cutting forces, their

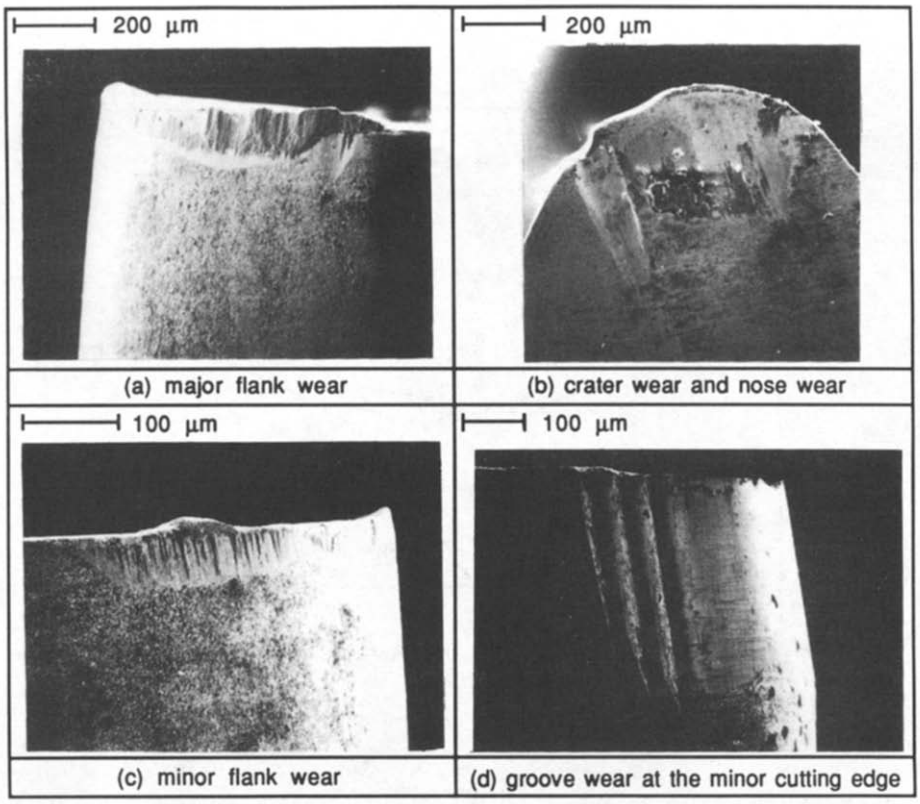

FIG. 1. Tool wear observed under scanning electron microscopy (SEM).

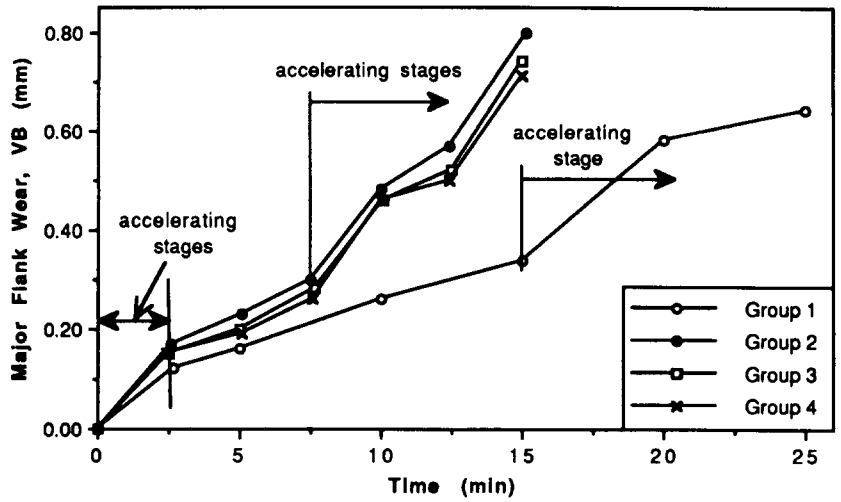

FIG. 2. Development of major flank wear.

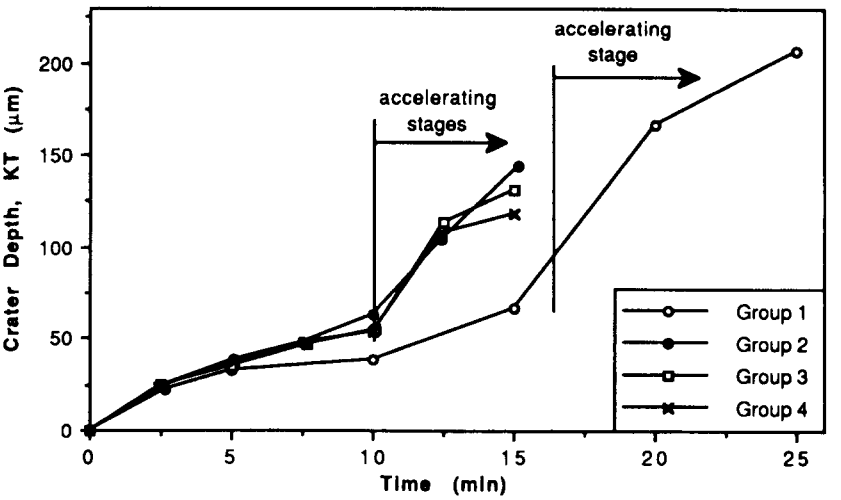

FIG. 3. Development of crater depth.

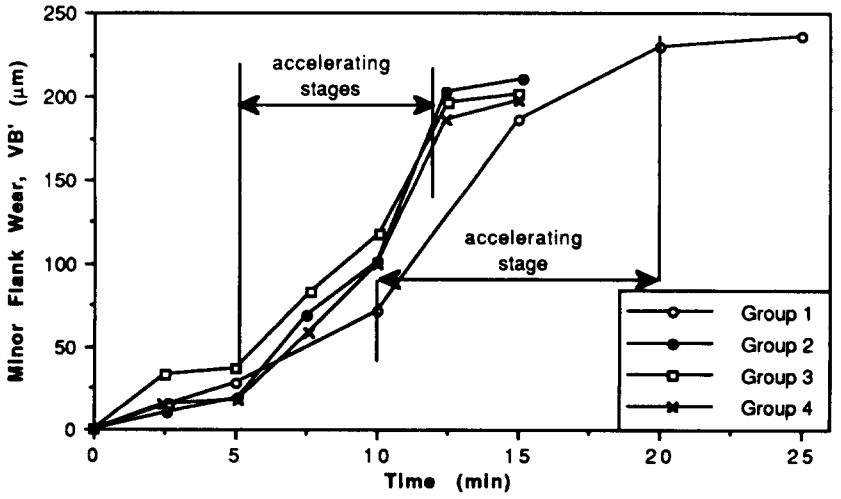

FIG. 4. Development of minor flank wear.

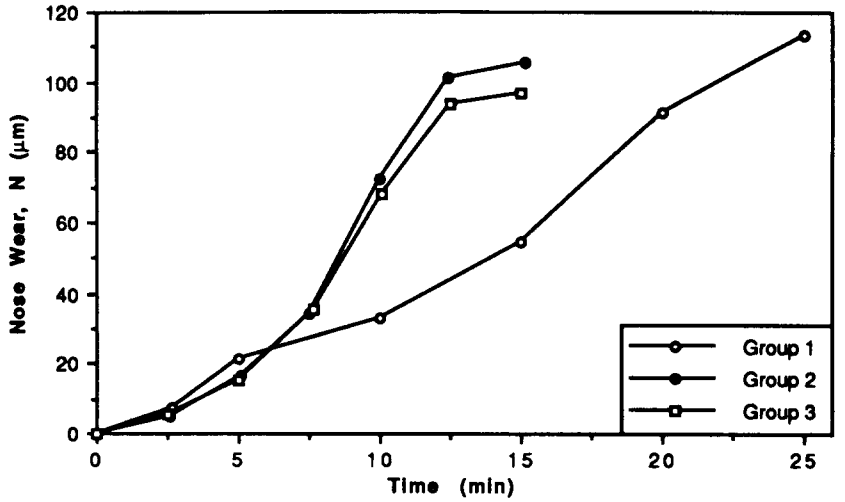

FIG. 5. Development of nose wear.

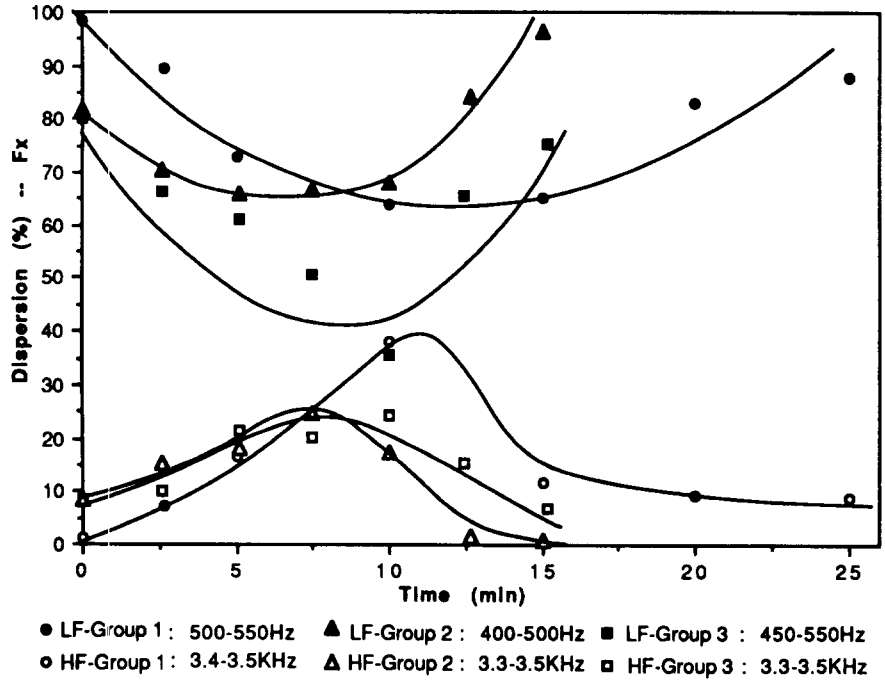

FIG. 6. Dispersion patterns in feed direction for groups 1–3.

relationships are illustrated in Fig. 9. Taking cutting condition group 1 as an example, the following results are presented.

In the feed direction, the feed force F_x is primarily associated with the normal force acting on the major flank $F_{\alpha n}$ and the horizontal friction force acting on the minor flank $F_{\beta h}$. Therefore, the tool/workpiece interactions on both flanks should be reflected in the dynamic feed force characteristics. By examining the LF dispersion curve for group 1, shown in Fig. 6, it was found that dispersion percentage values decrease to a minimum value between 10 and 15 min, while at the same time, major flank wear, VB (Fig. 2), arrives at its critical point for replacement (VB=0.35 mm) and after 15 min VB enters its accelerating stage. Thus, the behaviour of the LF dispersions is in agreement with the well-known rate of major flank wear curves. By comparing the HF dispersion curve for group 1 (Fig. 6) with the minor flank wear, VB' curve shown in Fig. 4, it is again found the former resembles the rate of the latter. The acceleration

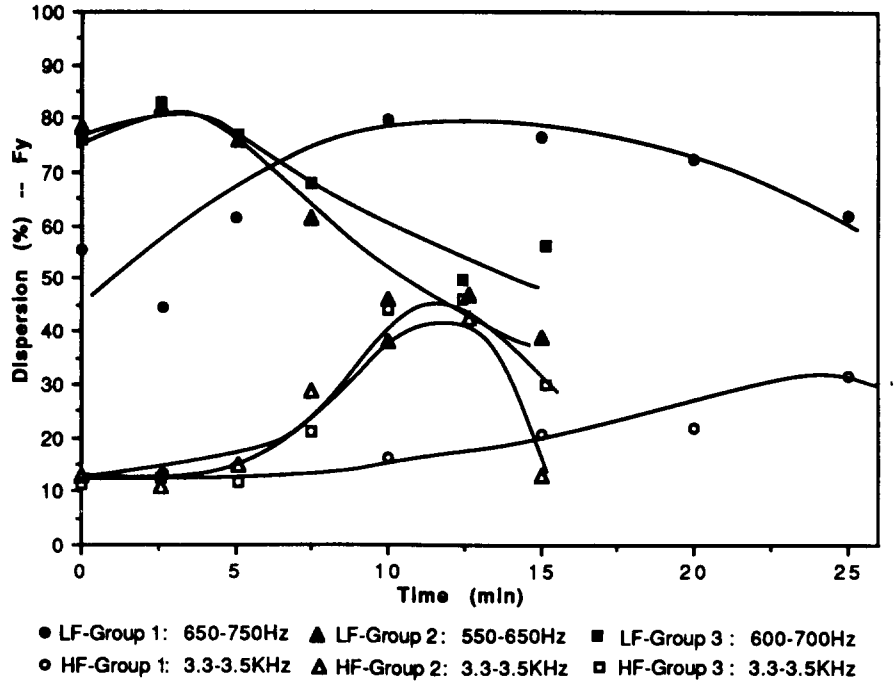

FIG. 7. Dispersion patterns in thrust direction for groups 1–3.

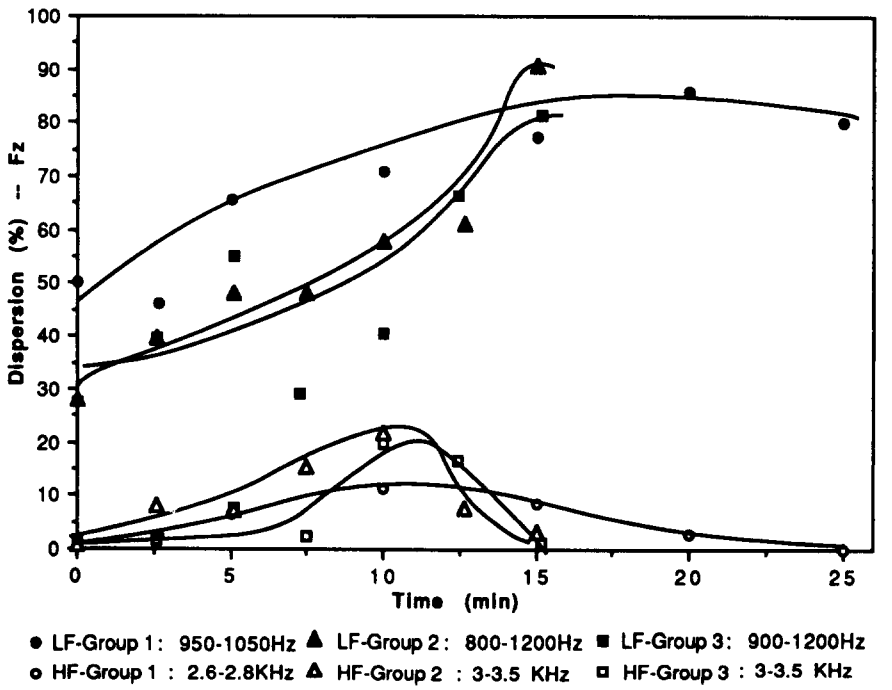

FIG. 8. Dispersion patterns in main cutting direction for groups 1–3.

of VB' at about 10 min could be detected by the maximum value of the HF dispersions.

In the thrust direction, the small depth of cut used in finish-machining produces a large chip flow angle such that the rake face friction force, F_γ, is almost along the thrust direction. Therefore, the thrust force F_y is associated with the normal force acting on the minor flank $F_{\beta n}$ and the friction force acting on the rake face F_γ. In a similar way, LF dispersion for group 1, shown in Fig. 7, can be related to the rate of

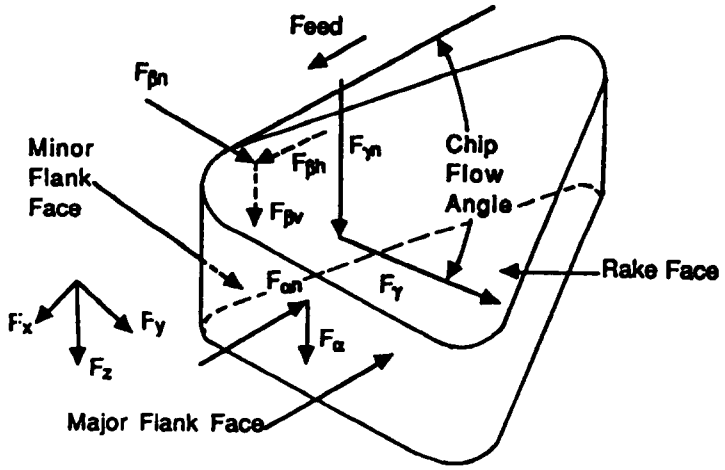

FIG. 9. Models for the forces acting on different tool faces.

minor flank wear VB' in Fig. 4 and HF dispersion to the rate of crater depth KT shown in Fig. 3.

In the main cutting direction, the dynamic cutting force, F_z, is primarily associated with the normal force acting on the rake face $F_{\gamma n}$, the friction force acting on the major flank F_α and the vertical friction force on the minor flank $F_{\beta v}$. By examining the LF and HF dispersions shown in Fig. 8, it was found that they reflect the rate of the crater wear and the minor flank wear shown in Figs 3 and 4, respectively. No recognizable trends which are associated with the friction force acting on the major flank F_α were found.

It is interesting to note that trends of LF dispersions, isolated from all three dynamic components of the cutting force, reflect the wear rate associated with normal forces, and the HF dispersions with tangential friction forces. As a summary, the interrelationships among them are given in Table 3.

3.4. *Strategies of tool wear estimation*

3.4.1. *Major flank wear.* Based on the discussion above, it can be concluded that the LF dispersion of feed force F_x is in agreement with the rate patterns of major flank wear VB, thus giving a good indication for the major flank wear.

3.4.2. *Minor flank wear.* Among the three dispersion patterns for the minor flank wear, i.e. the LF dispersion of F_y (Fig. 7), the HF dispersion of F_x (Fig. 6) and the HF dispersion of F_z (Fig. 8), the last two are found to exhibit a consistant pattern under all the three cutting conditions, groups 1–3. The HF dispersion of F_x, however, is more a static than a dynamic one, because of the slow feed motion. Therefore, HF dispersion of F_z can be used as the main indicator of the minor flank wear VB', and the HF dispersion of F_x as an auxiliary one. When one of them reaches the maximum, the accelerated minor flank wear is indicated.

3.4.3. *Crater wear.* For the crater depth, it can be seen that both LF dispersion of F_z and HF dispersion of F_y under all the three cutting conditions, groups 1–3, reach

TABLE 3. INTERRELATIONSHIPS AMONG THE FORCES, TOOL WEAR AND DISPERSION

F_x	$F_{\alpha n}$	(normal to major flank)	↔	VB	↔	LF dispersions
	$F_{\beta h}$	(tangential to minor flank)	↔	VB'	↔	HF dispersions
F_y	$F_{\beta n}$	(normal to minor flank)	↔	VB'	↔	LF dispersions
	F_γ	(tangential to crater face)	↔	KT	↔	HF dispersions
F_z	$F_{\gamma n}$	(normal to crater face)	↔	KT	↔	LF dispersions
	$F_{\beta v}$	(tangential to minor flank)	↔	VB'	↔	HF dispersions
	F_α	(tangential to major flank)	No recognizable trend was found			

their maximum values as the crater depth, KT, falls into the accelerating stage. Thus, both of them could be used as an indicator for the detection of the accelerating state of the crater depth.

From the characteristics test of machine-tool structural dynamics and idle disturbances, it is revealed that the frequencies of all HF dispersions are reasonably close to the natural frequencies of the tool holder/dynamometer system in each direction, while the ones of all LF dispersions are close to the machine-tool idle frequencies. Thus, the identification of physical nature for LF and HF dispersion provides the method of dispersion diagnosis with a reliable basis for comprehensive tool wear estimation in finish-turning.

4. ESTIMATION OF GROOVE WEAR AT MINOR CUTTING EDGE

Under certain cutting conditions, grooves may form at the minor cutting edge. It was found that once the groove wear occurs, the surface finish deteriorates dramatically [21–24, 30]. Therefore, it is obvious that for finish-turning, monitoring of the minor flank, major flank and crater wear is not sufficient, and monitoring of the groove wear at the minor cutting edge must be incorporated. Since the groove wear often induces high frequency vibration, a 3-D vibration signal is chosen for monitoring purposes.

4.1. *Groove wear experiments*

The multivariate vibration signals produced in the machining were sensed by a miniature 3-D accelerometer, PCB Model 306A06, mounted at the close vicinity of the tool tip. Table 4 shows the machining conditions used in the groove wear experiments, which are all within the range recommended by the cutting tool manufacturer.

In order to measure groove wear and surface roughness, the machining process was interrupted periodically. A set of 524 data points, with a sample interval equal to 30 μs, was taken for each of the three orthogonal directions, just before each interruption. An extra set of data was also recorded between consecutive interruptions to provide more information for signal processing. Scanning electron microscopy (SEM) was used as a major means to determine the groove wear. Surface roughness (R_a) was measured by using a portable surface measurement instrument.

4.2. *Patterns of groove wear at the minor cutting edge*

If the four cutting conditions selected in the experiments are classified into two groups, i.e. a lower feed (0.04 mm/rev) group for cutting condition groups B and D and a higher feed (0.08 mm/rev) group for cutting condition groups A and C, it can be seen there exist two different patterns, described as follows.

4.2.1. *Pattern of groove wear for the lower feed group.* A set of SEM photographs indicating four typical stages of groove wear development, i.e. initial, steady, severe and disappearance, is shown in Fig. 10 using group B as a representative. It is clear that at the severe stage of groove wear, the grooves were wiped out (Fig. 10(c)), indicating severe induced vibration. The changes in the number of grooves and surface roughness were further plotted in Fig. 11. It is apparent that the surface finish was sharply deteriorating when the grooves were being wiped out.

TABLE 4. MACHINING CONDITIONS USED IN GROOVE WEAR EXPERIMENTS

Machine tool	HITEC-20SII CNC Lathe (18 kW)
Tool insert type	TNMG160408 (Carbide P10, Grooved Chip Former)
Tool Geometry	0°, 5°, −6°, 90°, 60°, 0.8
Work material	AISI4140 (HNB=320)
Cutting conditions	Group A: V=160 m/min f=0.08 mm/rev d=0.25 mm
	Group B: V=160 m/min f=0.04 mm/rev d=0.25 mm
	Group C: V=190 m/min f=0.08 mm/rev d=0.25 mm
	Group D: V=190 m/min f=0.04 mm/rev d=0.25 mm

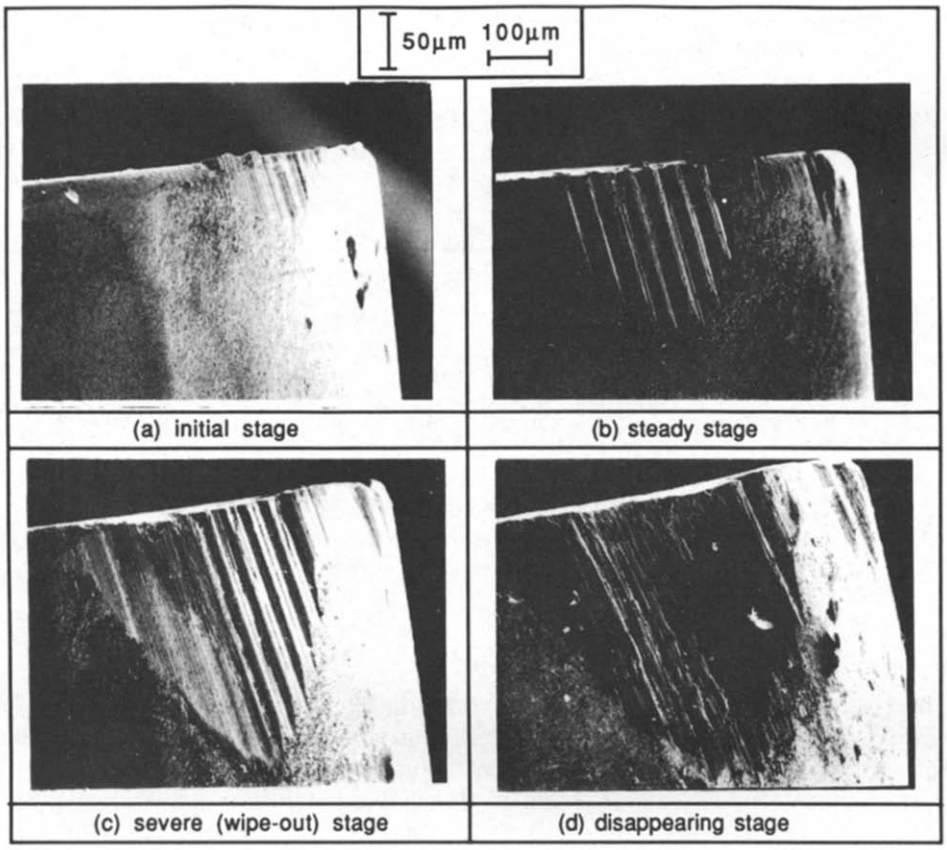

FIG. 10. Groove wear development for cutting condition group B.

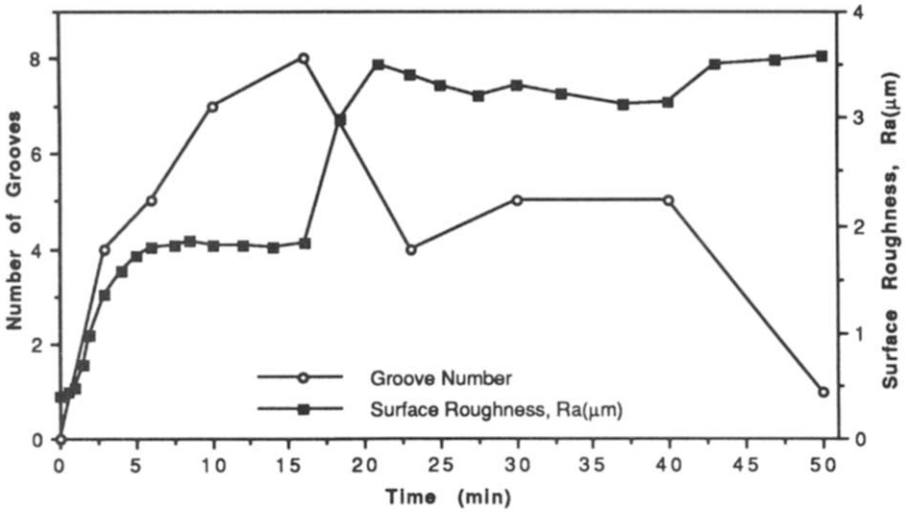

FIG. 11. The number of grooves and surface roughness for group B (cutting conditions: $V=160$ m/min, $f=0.04$ mm/rev, $d=0.25$ mm).

4.2.2. *Pattern of groove wear for the higher feed group.* Taking group A as a representative, the changes in the number of grooves and the surface roughness were plotted in Fig. 12. No decrease in the number of grooves and sharp increase in roughness occurred, even after machining for more than 50 min.

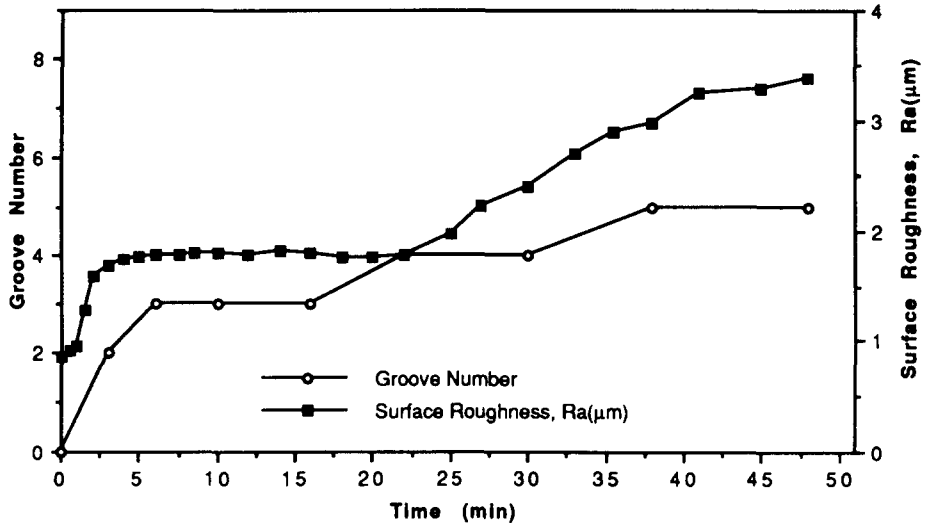

FIG. 12. The number of grooves and surface roughness for group A (cutting conditions: V=160 m/min, f=0.08 mm/rev, d=0.25 mm).

4.3. *Analysis based on dispersion patterns*

The preliminary analysis from the raw vibration signals shows that when the number of groove decreases, the signals exhibit different appearances. More detailed results, based on quantitative analysis and physical interpretation of the vibration behaviour, are required to formulate a more realistic yet reliable criterion. Dispersion analysis was concentrated on the lower feed group (0.04 mm/rev) as it describes the entire process of the development of groove wear at the minor cutting edge. There are two clear patterns of dispersions. One in the thrust direction, D_y with 9.3 kHz frequency and the other in the main cutting direction, D_z with 2.5 kHz frequency were found, being related to the development patterns of groove wear. The developments of these two dispersions for cutting condition group B were plotted in Fig. 13. Analysing Fig. 13, together with Fig. 11, which shows the groove development, it is seen that the dispersions, D_y and D_z, reached their maximum values when the number of grooves was decreasing, indicating the appearance of the severe vibrations under frequencies of 9.3 kHz in the thrust direction and 2.5 kHz in the main cutting direction. No recogni-

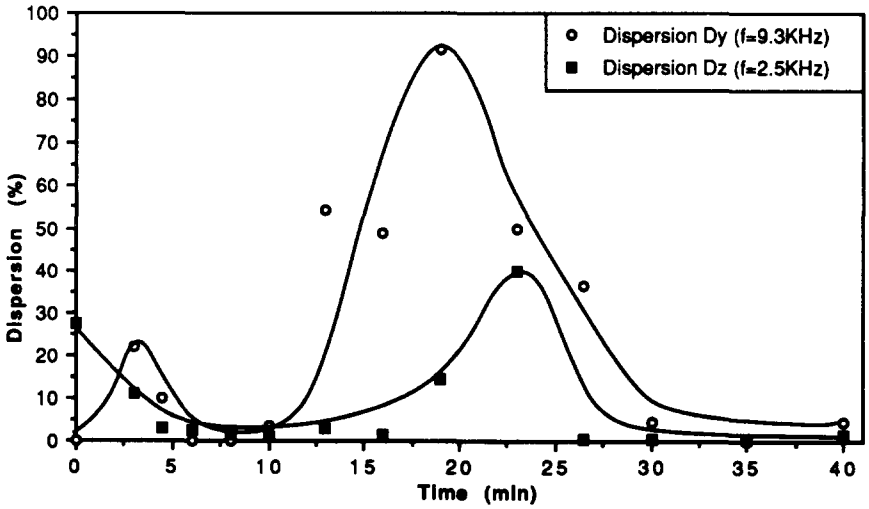

FIG. 13. The development of dispersion for group B.

zable dispersion trends were found in the analysis of vibration signal for the feed direction. By using conventional excitation tests, it was revealed that the frequencies of D_y and D_z are corresponding to natural frequencies of tool/holder, around 9340 Hz in thrust direction and 2610 Hz in main cutting direction respectively.

4.4. *Strategy of groove wear estimation*

As seen from the above analysis, the dispersions of D_y and D_z are sensitive to the decrease of groove number, and thus the deterioration of the surface finish. Comparing the developments of these two dispersion patterns, it is found that the occurrence of the D_z peak was about 3 min later than that of the D_y peak and the latter actually corresponds to the starting of groove wipe-out. This may indicate that severe vibration occurring in the thrust direction disturbs the regular grooves formed at the minor cutting edge. The disturbed minor cutting edge in turn excites vibration in the main cutting direction. Therefore, the strategy for estimating groove wear shall be the detection of the peak values of D_y and D_z.

5. CONCLUSION

The results presented in this paper represents an attempt to develop an overall tool wear monitoring strategy for finish-turning. It was shown that in order to estimate various types of wear development on different faces of a tool insert, multi-dimensional signals are required. Furthermore, an effective modelling technique is required. It is also shown that under certain conditions, the importance of monitoring groove wear at the minor cutting edge surpasses that of other types of wear.

Dispersion analysis, based on multivariate ARMA vector time series models was used to quantitatively describe the relative importance of modes of force and vibration variations. The merit of the method is its ability to isolate the ingredients from the dynamic cutting forces and vibration, each of which is sensitive to a particular wear state, thereby providing an overall yet sensitive tool wear estimation strategy for finish-turning. The relationships between the dispersion patterns and the particular types of tool wear are physically interpreted in terms of dynamic characteristics of the machining system.

The purpose of this paper is to establish relationships between the off-line measurements of tool wear and the dispersions based on 3-D dynamic cutting forces and/or 3-D vibrations measured in finish-machining, such that the tool wear monitoring strategy could be implemented in real-time.

REFERENCES

[1] D. Li and J. Mathew, Tool wear and failure monitoring techniques for turning—a review, *Int. J. Mach. Tools Manufact.* **30,** 579–598 (1990).
[2] J. Tlusty, A critical review of sensors for unmanned machining, *Ann. CIRP* **32,** 563–572 (1983).
[3] H. K. Toenshoff, J. P. Wulfsberg, H. J. J. Kals and W. Koenig, Developments and trends in monitoring and control of machining processes, *Ann. CIRP* **37,** 611–622 (1988).
[4] M. Shiraishi, Scope of in-process measurement, monitoring and control techniques in machining processes—Part 1: in-process techniques for tools, *Precision Engng* **10,** 179–189 (1988).
[5] S. Y. Liang and D. A. Dornfeld, Detection of cutting tool wear using adaptive time series modeling of acoustic emission signal, *ASME/WAM, Sensors for Mfg* **26,** 27–38 (1987).
[6] S. Y. Liang and D. A. Dornfeld, Tool wear detection using time series analysis of acoustic emission, *J. Engng Ind* **111,** 199–205 (1989).
[7] S. M. Pandit, H. Susuki and C. H. Kahng, Application of data dependent systems to diagnostic vibration analysis, *J. mech. Des.* **102,** 233–241 (1980).
[8] S. M. Pandit and S. Kashou, A Data dependent systems strategy of on-line tool wear sensing, *J. Engng Ind.* **104,** 217–223 (1982).
[9] D. A. Dornfeld, Neural network sensor fusion for tool condition monitoring, *Ann. CIRP* **39,** 101–105 (1990).
[10] Z. J. Yuan, Y. X. Yao and P. Yao, In-process detection of tool wear and breakage by autocorrelation coefficient of dynamic cutting forces in turning, *Proc. 4th Int. Conf. on Mfg Engng,* pp. 201–205, Brisbane, Australia (1988).
[11] A. M. Petrie, T. S. Sifra and A. Ismail, The development of an automated system for on-line tool wear monitoring, *Proc. of 1st Int. Machinery Monitoring and Diagnostics Conf.,* pp. 546–552, U.S.A. (1989).

[12] Y. KOREN, K. DANAI, A. G. ULSOY and T. R. KO, Monitoring tool wear through force measurement, *Proc. of 15th North American Manufacturing Research Conf.* pp. 463–468 (1987).
[13] S. B. RAO, Tool wear monitoring through the dynamics of stable turning, *Trans. ASME, J. Engng Ind.* **108,** 183–190 (1986).
[14] J. VOGEL, S. PAMALINGAM and K. STELSON, On tool post vibration monitoring for tool condition identification, *Proc. of 14th North American Manufacturing Research Conf.* pp. 281–285 (1986).
[15] G. CHRYSSOLOURIS, M. GUILLOT and M. DOMROESE, Tool wear estimation for intelligent machining, *ASME/WAM, Intelligent Control* **5,** 35–43 (1987).
[16] F. GIUSTI, M. SANTOCHI and G. TANTUSSI, On-line sensing of flank and crater wear of cutting tools, *Ann. CIRP* **36,** 41–44 (1987).
[17] R. TETI, Tool wear monitoring through acoustic emission, *Ann. CIRP* **38,** 99–102 (1989).
[18] K. DANAI and A. G. ULSOY, A dynamic state model for on-line tool wear estimation in turning, ASME/WAM, *Sensors and Control for Mfg* **18,** 137–148 (1985).
[19] A. J. PEKELHARING and C. A. VAN LUTTERVELT, *CIRP Terminology and Procedures for Turning Research* p. 77. Technical Secretary CIRP group C, Delft (1969).
[20] K. OKUSHIMA, K. HITOMI and S. ITO, A study of super-high speed machining, *Ann. CIRP* **13,** 399–410 (1966).
[21] A. J. PEKELHARING and R. A. SCHUERMANN, Wear of carbide tools—its effect on surface finish and dimensional accuracy, *The Tool Engineer*, pp. 51–57 (Oct. 1953).
[22] A. J. PEKELHARING, Finish turning, *Ann. CIRP* **8,** 112–120 (1959).
[23] B. H. LAMBERT, Two years of finish-turning research at the Technological University, Delft, *Ann. CIRP* **10,** 246–255 (1961–62).
[24] A. J. PEKELHARING, Some special aspects of carbide tool wear, *Int. Prod. Engng Res. Conf.* ASME, New York (1963).
[25] S. TAKATA and T. SATA, Model referenced monitoring and diagnosis—application to manufacturing system, *Computers in Industry* **7,** 31–43 (1986).
[26] K. EMAN and S. M. WU, A feasibility study of on-line identification of chatter in turning operations, *J. Engng Ind.* **102,** 315–321 (1980).
[27] X. D. FANG, Y. YAO and G. ARNDT, Tool wear estimation by multidimensional autoregressive spectral analysis, *Proc. 1990 Pacific Conf. on Mfg* Vol. 2, pp. 834–841 Sydney and Melbourne, Australia (1990).
[28] Y. YAO, X. D. FANG and G. ARNDT, Comprehensive tool wear estimation in finish-machining via multivariate time-series analysis of 3-D cutting forces, *Ann. CIRP* **39,** 57–60 (1990).
[29] S. M. PANDIT, Analysis of vibration records by data dependent systems, *Shock and Vibr. Bull.* **47,** 161–174 (1977).
[30] Y. YAO, X. D. FANG and G. ARNDT, On-line estimation of groove wear in the minor cutting edge for finish-machining, accepted for publication in *Ann. CIRP* **40**/1 (1991).
[31] P. BANDYOPADHYAY and S. M. WU, Signature analysis of drilling dynamics for on-line drill life monitoring, ASME/WAM, *Sensors and Controls for Mfg* **18,** 101–110 (1985).
[32] M. S. LAN and Y. NAERHEIM, In-process detection of tool breakage in milling, *Trans ASME, J. Engng Ind.* **108,** 191–197 (1986).
[33] S. M. PANDIT and S. M. WU, *Time Series and System Analysis with Applications*. Wiley, USA (1983).
[34] B. MILLS and A. H. REDFORD, *Machinability of Engineering Materials*, p. 172. Applied Science Publishers (1983).